Roles of Cysteine 161 and Tyrosine 154 in the Lecithin−Retinol Acyltransferase Mechanism†

Linlong Xue and Robert R. Rando*

Department of Biological Chemistry and Molecular Pharmacology, Harvard Medical School, 45 Shattuck Street, Boston, Massachusetts 02115

Received March 5, 2004; Revised Manuscript Received March 30, 2004

ABSTRACT: Lecithin−retinol acyltransferase (LRAT) catalyzes the transfer of an acyl moiety from the *sn*-1 position of lecithin to vitamin A, generating all-*trans*-retinyl esters. LRAT is a unique enzyme and is the founder member of an expanding group of proteins of largely unknown function. In an effort to understand the mechanism of LRAT action, it was of interest to assign the amino acid residues responsible for the two pK_a values of 8.22 and 9.95 observed in the pH vs rate profile. Titrating C161 of LRAT with a specific affinity labeling agent at varying pH values shows that this residue has a pK_a = 8.03. Coupled with previous studies, this titration reveals the catalytically essential C161 as the residue responsible for the ascending limb of the pH vs rate profile. Site-specific mutagenic experiments on the lysine and tyrosine residues of LRAT reveal that only the highly conserved tyrosine 154 is essential for catalytic activity. This residue is likely to be responsible for the pK_a = 9.95 found in the pH vs rate profile. Thus, LRAT has three essential residues (C161, Y154, and H60), all of which are conserved in the LRAT family of enzymes.

Lecithin−retinol acyltransferase (LRAT)[1] catalyzes the reversible acylation of vitamin A and isomers using lecithin as an acyl donor to generate the corresponding retinyl esters (Scheme 1) (*1*−*4*). The enzyme is essential in the visual cycle because all-*trans*-retinyl esters, the acylation product of vitamin A, are the substrates for an isomerohydrolase enzyme which processes them into 11-*cis*-retinol (*5*, *6*). The 11-*cis*-retinol is subsequently oxidized to 11-*cis*-retinal, the chromophore of rhodopsin (*4*). As expected, a mouse LRAT knockout is unable to synthesize 11-*cis*-retinoids (*7*). LRAT is also important in the general nutritional processing of vitamin A (*8*). On a molecular level, the primary sequence of the enzyme is novel and is the founder member of a large cohort of presumed enzymes of unknown function (*9*). This cohort includes class II tumor supressors, a putative enzyme EGL-26 essential in *Caenorhabditis elegans* morphogenesis, and a group of putative viral proteases (*10*−*13*). That LRAT might have a novel protease motif would not be considered unusual because the reaction that it catalyzes is similar to a hydrolysis reaction, except that the attacking nucleophile is retinol rather than H_2O. Indeed, the kinetic mechanism of LRAT involves an ordered ping-pong process with acylation of an active site nucleophile with lecithin to generate an acyl-enzyme intermediate and a 2-acylphospholipid (*14*). The acyl group is then accepted by vitamin A to generate all-*trans*-retinyl esters (*15*).

Site-specific mutagenic experiments on LRAT have identified two essential residues, C161 and H60, implying a thiol protease (lipase) mechanism of the papain family, with C161 serving as the active site nucleophile (*9*, *16*). These forementioned residues are conserved in the LRAT family (*9*). However, the similarity to the papain family ends here both because of the lack of sequence homology to this family and because of apparent mechanistic dissimilarities. For example, the well-studied papain family shows two apparent pK_a values of 4.0 and 8.5, while LRAT has apparent pK_a values of 8.5 and 10.4 (*16*). In the papain series, the lower pK_a is assigned to the active site cysteine and the second pK_a to the histidine residue (*17*). In the case of LRAT, one can speculate that the pK_a = 8.5 might be assigned to the active site cysteine residue C161, because a pK_a of this magnitude is in line with expectations for a thiol (*14*). However, as the assignment of a pK_a = 4 to the thiol nucleophile of papain makes clear, active site residues may have pK_a values considerably different from expectations (*17*). Therefore, it was of some interest to precisely assign the two relevant pK_a values of LRAT to further define the mechanistic class of the LRAT family of enzymes. In the current studies, a truncated form of LRAT (tLRAT) is investigated because tLRAT can be expressed in bacteria and purified to homogeneity (*18*). The studies reported here show that the pK_a of approximately 8 in LRAT is indeed that of C161. Moreover, the pK_a of approximately 10 is assigned to Y154, acting as an acid in the catalytic reaction.

EXPERIMENTAL PROCEDURES

Materials

The synthesis of 3-[*N*-boc-Lys(biotinyl)-*O*]-all-*trans*-retinyl chloroacetate (BRCA) is described elsewhere (*19*). The sample of BRCA used was a generous gift of Prof. Koji

† The work described here from the authors' laboratory was supported by the U. S. Public Health Service, NIH Grant EY-04096.

* To whom correspondence should be addressed. Phone: (617) 432-1794. Fax: (617) 432-0471. E-mail: robert_rando@hms.harvard.edu.

[1] Abbreviations: BSA, bovine serum albumin; DPPC, L-α-dipalmitoylphosphatidylcholine; LRAT, lecithin−retinol acyltransferase; BRCA, 3-[*N*-boc-Lys(biotinyl)-O]-all-*trans*-retinyl chloroacetate; DTT, dithiothreitol; EDTA, ethylenediaminetetraacetic acid disodium salt; IPTG, isopropyl β-D-thiogalactopyranoside; DMSO, dimethyl sulfoxide; SDS−PAGE, sodium dodecyl sulfate−polyacrylamide gel electrophoresis.

10.1021/bi049556f CCC: $27.50
Published on Web 05/01/2004

Scheme 1: Mammalian Visual Cycle

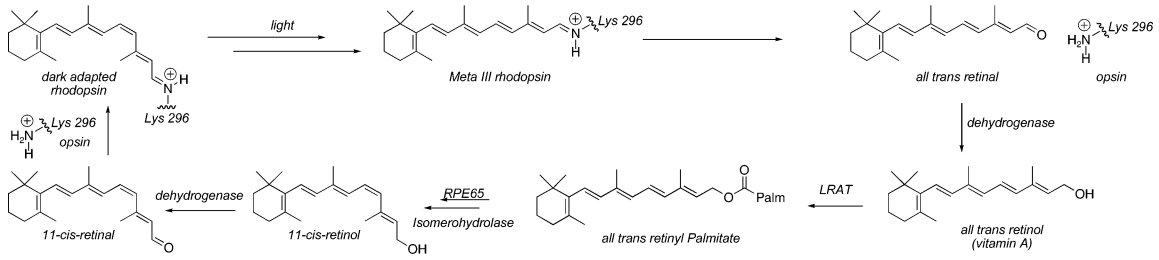

Table 1: Primers for Site-Directed Mutagenesis of TLRAT

K90A	(+): 5′-GGG CGC ACG CAG GCG GTG GTC TCC AAC-3′
	(−): 5′-GTT GGA GAC CAC CGC CTG CGT GCG CCC-3′
K95A	(+): 5′-TG GTC TCC AAC GCG CGT CTC ATC CTG-3′
	(−): 5′-CAG GAT GAG ACG CGC GTT GGA GAC CAC-3′
K104A	(+): 5′-CTG GGC GTT ATT GTC GCA GTG GCC AGC ATC-3′
	(−): 5′-GAT GCT GGC CAC TGC GAC AAT AAC GCC CAG-3′
K133A	(+): 5′-C GAG TCC CTC CAG GCA AAG GCA CTG CTC CAA CGA G-3′
	(−): 5′-C TCG TTG GAG CAG TGC CTT TGC CTG GAG GGA CTC G-3′
K134A	(+): 5′-C GAG TCC CTC CAG AAA GCG GCA CTG CTC CAA CGA G-3′
	(−): 5′-C TCG TTG GAG CAG TGC CGC TTT CTG GAG GGA CTC G-3′
K133A/K134A	(+): 5′-C GAG TCC CTC CAG GCA GCG GCA CTG CTCC AAC GAG-3′
	(−): 5′-C TCG TTG GAG CAG TGC CGC TGC CTG GAG GGA CTC G-3′
K147A	(+): 5′-CGG AGG GCT GAA GCG CTG CTG GGC TTT-3′
	(−): 5′-AAA GCC CAG CAG CGC TTC AGC CCT CCG-3′
K180A	(+): 5′-T CCC CAG TCC GAC GCG TTT TGT GAG ACT G-3′
	(−): 5′-C AGT CTC ACA AAA CGC GTC GGA CTG GGG A-3′
K180R	(+): 5′-T CCC CAG TCC GAC AGG TTT TGT GAG ACT G-3′
	(−): 5′-C AGT CTC ACA AAA CCT GTC GGA CTG GGG A-3′
K186A	(+): 5′-TTT TGT GAG ACT GTG GCG ATA ATT ATT CGT GAT-3′
	(−): 5′-ATC ACG AAT AAT TAT CGC CAC AGT CTC ACA AAA-3′
K186R	(+): 5′-TTT TGT GAG ACT GTG AGG ATA ATT ATT CGT GAT-3′
	(−): 5′-ATC ACG AAT AAT TAT CCT CAC AGT CTC ACA AAA-3′
Y64F	(+): 5′-C CAC TAT GGC ATC TTC CTA GGA GAC AAC C-3′
	(−): 5′-G GTT GTC TCC TAG GAA GAT GCC ATA GTG G-3′
Y118F	(+): 5′-GAG GAC TTC GCC TTC GGA GCT AAC ATC C-3′
	(−): 5′-G GAT GTT AGC TCC GAA GGC GAA GTC CTC-3′
Y154F	(+): 5′-GGC TTT ACC CCC TTC AGC CTG CTG TGG-3′
	(−): 5′-CCA CAG CAG GCT GAA GGG GGT AAA GCC-3′
Y167F	(+): 5′-G CAC TTC GTG ACC TTC TGC AGA TAT GGC A-3′
	(−): 5′-T GCC ATA TCT GCA GAA GGT CAC GAA GTG C-3′

Nakanishi of Columbia University. Frozen bovine eye cups were obtained from W. L. Lawson Co. (Lincoln, NE). Western blot blocking buffer, Gel-code blue, and Tris-buffered saline pack (25 mM Tris, 150 mM NaCl, pH 7.2) were from Pierce. HPLC-grade solvents were from J. T. Baker. Coomassie brilliant blue R-250 was from Bio-Rad. The silver staining kit, polyvinylidene fluoride membrane, anti-rabbit Ig conjugated horseradish peroxidase, and the ECL-Western blotting kit were from Amersham Pharmacia Biotech. Precast gels (4−20%, 8 cm × 8 cm) for SDS−PAGE and *Escherichia coli* BL21STAR (DE3) competent cells were from Invitrogen Life Technologies. Benchmark prestained markers were from GibcoBRL Life Technologies. Biotinylated molecular mass markers, two-color prestained markers, avidin-conjugated horseradish peroxidase, and 10× Tris-buffered saline solution (20 mM Tris, 500 mM NaCl, pH 7.5) were from Bio-Rad. [11,12-$^3H_2$]-All-*trans*-retinol was obtained from NEN Life Sciences. L-α-Dipalmitoylphosphatidylcholine (DPPC), bovine serum albumin (BSA), and dithiothreitol (DTT) were from Sigma. The QuikChange site-directed mutagenesis kit was purchased from Stratagene. Anti-LRAT antibody was a generous gift of Prof. Dean Bok (UCLA). The wild-type expression vectors for tLRAT were also gifts of Prof. Bok. All other reagents were of analytical grade.

Methods

Site-Directed Mutagenesis. tLRAT mutants were prepared using a QuikChange site-directed mutagenesis kit (Stratagene Inc.) according to the vendor's instruction with minor modifications. The primers used for tLRAT mutagenesis are listed in Table 1. The mutants were verified by DNA sequencing before expression and Western blot using anti-LRAT antibody after expression.

Protein Expression and Purification. For wt tLRAT and mutants, the plasmids pET15b containing tLRAT genes were transformed into *E. coli* BL21STAR (DE3) cells for expression. Briefly, the cells were grown in LB media containing 1 mg/L ampicillin at 37 °C with shaking at 275 rpm. When the OD_{600nm} reached 0.8, IPTG (final concentration 1 mM) was added to induce expression. Cells were harvested 4−6 h after induced expression and stored at −80 °C. The expressed protein was extracted with 1% SDS at room temperature after the cells were lysed either with lysozyme or by sonication. Protein purification was accomplished by applying the SDS extract directly onto a Ni^{2+}-NTA column as described (*18*), followed by dialysis against 100 mM sodium phosphate buffer (pH 7.4) containing 1 mM EDTA, 2 mM DTT, and 0.05% SDS. The protein concentration was determined by using the Bio-Rad D_C protein assay kit (Bio-Rad Inc.)

Activity Assay of tLRAT and the Mutants. The activity of tLRAT and mutants was followed by measuring all-*trans*-retinyl ester formation using 0.2 μM [11,12-$^3H_2$]-all-*trans*-retinol as substrate. The reaction mixture (100 mL) contained 100 mM Tris-HCl (pH 8.4), 1 mM EDTA, 1 mM DTT, 5 μM tLRAT, and 240 μM DPPC/BSA (0.6%). The reaction was initiated by adding all-*trans*-retinol and incubated at room temperature for 10 min. The reaction was stopped by the addition of 500 μL of methanol, followed by the addition of 100 μL of H_2O, after which 500 μL of hexane was used to extract the retinoids. The extract was subject to normal-phase HPLC (NP-HPLC) analysis as previously described (*20*).

pH-Dependent Kinetics of tLRAT. tLRAT activity was measured at different pH values. Tris-HCl buffers (100 mM) were used in the pH range of 7−9. Glycine−NaOH buffers (100 mM) were prepared for the pH range of 9−11. The reaction mixture (100 μL) contained 100 mM buffer of different pH, 1 mM EDTA, 1 mM DTT, 5 μM tLRAT, and 240 μM DPPC/BSA (0.6%). The reaction was initiated by adding [11,12-$^3H_2$]-all-*trans*-retinol (0.1, 0.2, 0.5, 0.7, 1.0, 1.5, 2.0, and 3.0 μM) and was incubated at room temperature for 10 min. Retinyl ester formation was determined as indicated above.

Reversible Inactivation of tLRAT. To measure reversible inactivation of tLRAT, tLRAT was incubated with pH 10.40 buffer (100 mM) for 1 h at room temperature. The sample was then divided into two parts, and half was used for the direct activity assay as described above. The other half was subjected to dialysis against pH 8.40 Tris-HCl buffer (100 mM) overnight, after which the activity was measured as described above. For all activity assays in this section, the substrate concentration of [11,12-$^3H_2$]-all-*trans*-retinol was 0.2 μM and the incubation time was 10 min at room temperature.

pH-Dependent Specific Labeling of tLRAT by BRCA. Affinity labeling protocols are described elsewhere (*9*, *20*, *21*). All labeling experiments using retinoids were performed in a dark room under dim red light. Generally, 100 μg of purified tLRAT (1 mg/mL) was incubated with BRCA (10 μM) in 100 mM buffers (pH varies from 3.03 to 11.03) for 1 h at 4 °C. At the end of the incubation period, protein was precipitated with acetone (1 mL, −20 °C), and the precipitate was dissolved in H_2O. The labeled sample was applied to a SDS−PAGE, Tris−glycine polyacrylamide gel (4−20%, 8 cm × 8 cm), and electrophoresis was carried out in Tris (25 mM), glycine (192 mM), and SDS (0.1%) running buffer. Protein was denatured by heating samples (100 °C, 2 min) in sample buffer (2×) containing SDS (4%), 2-mercaptoethanol (10%), glycerol (20%), bromophenol blue (0.004%), and Tris-HCl (125 mM, pH 6.8). Proteins were visualized by Coomassie staining (0.1%).

After separation by SDS−PAGE, the proteins were transferred to polyvinylidene fluoride (PVDF) membranes. Then membranes were blocked in the blocking solution (100 mL, 3% gelatin, 25 mM Tris, 150 mM NaCl, pH 7.2) using a shaker platform for 1 h. The blocking solution was removed, and the membrane was washed twice with TTBS solution (0.05% Tween 20, 25 mM Tris, 150 mM NaCl, pH 7.2) for 5 min. After the TTBS buffer was removed, avidin-conjugated horseradish peroxidase (33 μL) in antibody buffer (100 mL, 1% gelatin, 0.05% Tween 20, 25 mM Tris, 150 mM NaCl, pH 7.2) was applied for 1 h. The membrane was washed twice with TTBS (100 mL, 0.05% Tween 20, 25 mM Tris, 150 mM NaCl, pH 7.2) for 5 min and twice by TBS (100 mL, 25 mM Tris, 150 mM NaCl, pH 7.2) for 5 min. ECL solution (6 mL) was added into the membrane for 1 min before X-ray film exposure. Using a higher concentration of saline TTBS buffer (20 mM Tris, 0.05% Tween 20, 500 mM NaCl, pH 7.5) reduced the background signal of the endogenously biotinylated protein bands. The Western blot images (X-ray film exposure) were scanned and quantified using a GS-800 calibrated densitometer (Bio-Rad Inc.).

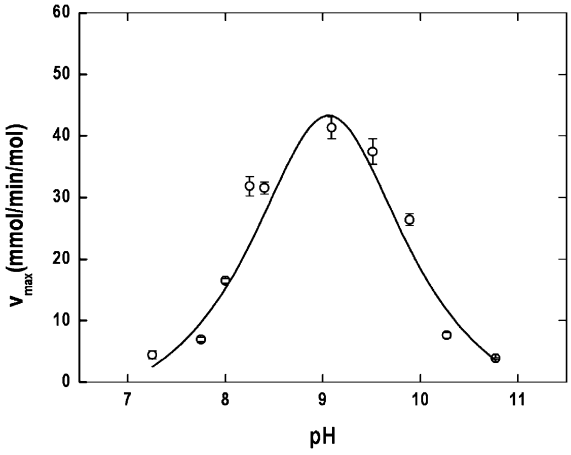

FIGURE 1: pH-dependent kinetics of tLRAT. The experiments were performed as indicated in the Methods section. tLRAT kinetics were measured at pH values of 7.25, 7.75, 8.0, 8.25, 8.40, 9.09, 9.51, 9.89, and 10.27. The V_{max} was derived from all-*trans*-retinol concentration-dependent kinetics of tLRAT, resulting in a V_{max} vs pH plot of tLRAT as shown in the figure. The two pK_a values calculated from pH-dependent kinetics of tLRAT are 8.22 and 9.95, respectively. All experiments were done in triplicate, and the errors are shown as error bars in the figure.

RESULTS

pH vs Rate Profile for tLRAT. The experiments carried out here were performed on tLRAT which contains residues 31−196 of LRAT deleting the N- and C-terminal hydrophobic membrane associated domains of LRAT (*18*). While we have not observed significant differences in behavior between LRAT and tLRAT, it is important for the current experiments to directly establish the pH vs rate profile for tLRAT. The pH vs rate profile for tLRAT is shown in Figure 1. The measured pK_a values are 8.22 and 9.95, which are quite similar to those measured for native LRAT (*16*). The higher pK_a = 9.95 is not observed in thiol proteases, so it is important to show that tLRAT is not simply denatured at higher pHs. In Figure 2 are shown data on the effects of incubation of tLRAT at pH = 8.40 where it is highly active. At pH = 10.40, the activity of LRAT is low, but even after incubation for 1 h at this pH, the subsequent lowering of the pH to 8.40 essentially restores full enzymatic activity. Therefore, tLRAT is not irreversibly denatured at high pH values, and this cannot be the reason for the decrease in activity at the higher pH values.

Titration of C161 with the Affinity Label BRCA. C161 is known to be the active site thiol residue of LRAT (*9*, *16*). This residue is specifically alkylated by the affinity labeling reagent BRCA shown in Scheme 2 (*9*). Since the reagent is

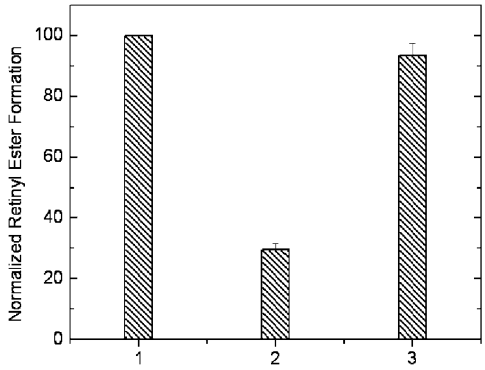

FIGURE 2: Reversible inactivation of tLRAT. The experiments were conducted as described in the Methods section. Bar 1 shows the activity of tLRAT at pH 8.40; bar 2 represents the activity of tLRAT at pH 10.40; bar 3 shows the activity of tLRAT samples which were first incubated at pH 10.40 for 1 h and then adjusted back to pH 8.40 by dialysis against 100 mM Tris-HCl buffer (pH 8.40) overnight at 4 °C. All experiments were done in triplicate, and the errors are shown as error bars in the figure.

biotinylated, labeling can be readily followed, and thus it should be possible to titrate C161 at various pH values with BRCA. Quantifying the extents of reaction as a function of pH generates a titration curve yielding an independent measurement for the pK_a of C161. As shown in Figure 3, when this is carried out, a smooth titration curve is generated with a measured pK_a = 8.03. From these data we conclude that the active site C161 can be assigned the pK_a = 8.22 observed in the pH vs rate profile for tLRAT.

Site-Specific Mutagenic Studies and Essential Nature of Y154. As shown in Figure 2, tLRAT is not irreversibly denatured at high pH values so that the measured higher pK_a may be of mechanistic significance. Lysine and tyrosine residues are under consideration as starting points for an investigation into the identification of a catalytically relevant amino acid residue with a potential pK_a of approximately 10. There are 12 Lys residues in human LRAT (Scheme 3), two of which (K2 and K15) are already missing in tLRAT and therefore are not essential residues. Of the remaining 10 Lys residues K95, K104, K133, and K180 are conserved in all of the six LRAT isoforms known (Scheme 3) (*4*). In Figure 4 are shown data for the K → A and K → R substitutions at these positions. It is clear from these data that Lys residues are not essential for function, even within the group of LRAT isoforms from different species.

LRAT contains seven Tyr residues (Y40, Y61, Y64, Y118, Y154, Y167, and Y214). Y40, Y61, and Y214 are not conserved in the LRAT family of proteins (Scheme 3). Of

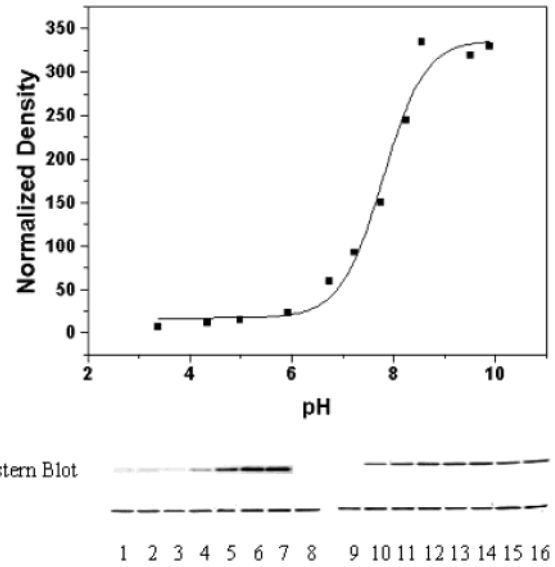

FIGURE 3: Affinity labeling of tLRAT by BRCA at different pH values. The experiments were performed as described in the Methods section. The affinity labeling of tLRAT by BRCA was measured at different pHs. The lower part of the figure shows the Coomassie-stained gel images and Western blot images of the samples at different pHs. Lanes: 1, pH 3.03; 2, pH 3.38; 3, pH 4.35; 4, pH 4.99; 5, pH 5.93; 6, pH 6.75; 7, pH 7.23; 8, pH 7.75; 9, pH 7.75; 10, pH 7.75; 11, pH 8.25; 12, pH 8.55; 13, pH 9.09; 14, pH 9.51; 15, pH 9.89; 16, pH 11.03. Among these, samples 8 and 9 are controls minus BRCA labeling. The exposure time was 30 s for the Western blot of samples 1−8 and 3 s for samples 9−16. The upper part of the figure shows the normalized signal density of the Western blot shown in the lower part. The results are the average of two separate experiments. The pH value at half of the maximal labeling (pK_a) is 8.03. The protein band of tLRAT appears at approximately 21 kDa by SDS−PAGE.

the remaining Tyr residues Y154 is the most highly conserved residue in the family (*9*). The remaining three Tyr residues (Y64, Y118, and Y167) of LRAT are generally conserved, though to a lesser extent than Y154. Consequently, we prepared the Y → F substituted tLRATs at positions 154, 64, 118, and 167 and determined their enzymatic activities (Figure 5). As revealed in this figure, only the F154 mutant proved to be inactive. This suggests that the conserved Y154 is essential for catalysis in the greater LRAT family of enzymes.

DISCUSSION

The studies reported here are aimed at revealing the amino acid residues of LRAT, with pK_a values of approximately 8.22 and 9.95, involved in the rate-limiting catalytic steps.

Scheme 2: Active Site Titration of LRAT

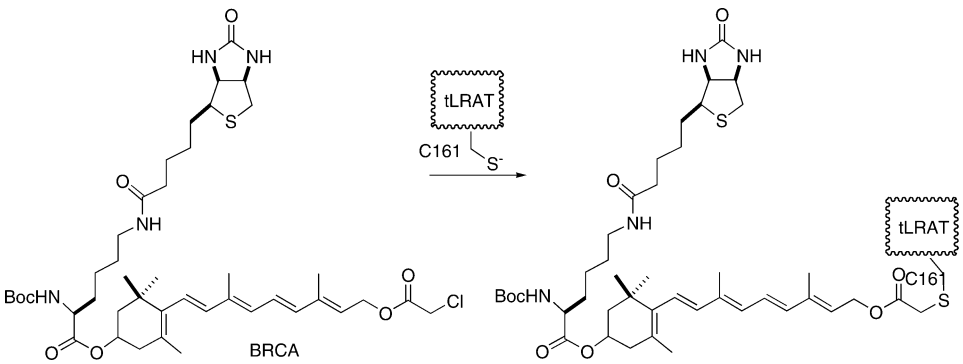

Scheme 3: Multiple Sequence Alignment of the LRAT Family[a]

```
Human-LRAT                        -MKNPMLEVVSLLLEKLLLISNFTLFSSGAAGKDKGRNSFYETS-SFHRG 48
Bovine-LRAT                       -MKNPMLEAVSLVLEKLLFISYFKFFSSGAPGQDKAGNTLYEIS-SFLRG 48
Mouse-LRAT                        -MKNPMLEAASLLLEKLLLISNFKLFSVSVPGGGTGKNRPYEIS-SFVRG 48
Rat-LRAT                          -MKNSMLEAASLLLEKLLLISNFKIFSVCAPGGGTGKKHPYEIN-SFLRG 48
XL-LRAT                           -MKSLLVGMIVFIFEKIFILANLKVFSVSS--KKSRCRQPCNVP-FIKRG 46
ZF-LRAT                           -----MLDSLSLLLEKTLLLAHFNFFSTTSSKQERCTKRREEISTYFQRG 45
HRev107-Mouse                     ------------------------------------MLAPIPEP---KPG 11
HREV107-RAT                       -------------------------------------MPIPEP---KPG 9
HRev107-3                         ------------------------------------MRAPIPEP---KPG 11
TIG3                              ------------------------------------MASPHQEP---KPG 11
Echovirus23                       KIEVYLSLRCPNLFFPSPAPKEKTSRALRGDLANFIDQSPYGQQQQTQMM 53
HumanParechovirus1                -----LSLRCPNFFFPLPAPKVTSSRALRGDMANLTNQSPYGQQPQNRMM 45
HumanParechovirus2                -----LSLRCPNFFFPLPAPKP-ATRKYRGDLATWSDQSPYGRQGKKQLM 44
Avian-encephalomyelitis-virus     -----------KTVMNTYWLDDDELVEESSHSSFDEIEEAQCSKCKMDLG 39
EGL26                             RLTTVLGRPGMFSFDDPPIGSQFPVGKELIQLDEVPVGVHDRQDKYLEKG 150
Aichivirus                        ---------------------------------------TPDVDP------ 6

Human-LRAT                        D----VLEVPRTHLTHYGIYLGDNRVAHMMPDILLALTDDMGRTQKVVSN 94
Bovine-LRAT                       D----VLEVPRTHLTHYGIYLGDNRVAHMMPDILLALTDDKGRTQKVVSN 94
Mouse-LRAT                        D----VLEVSRTHFIHYGIYLGENRVAHLMPDILLALTNDKERTQKVVSN 94
Rat-LRAT                          D----VLEVSRTHFTHYGIYLGDNRVAHLMPDILLALTSDKERTQKVVSN 94
XL-LRAT                           D----LLEVPRTLFVHFGIYLGNNKVAHLMPDILPALSDDTCLIRRVVTN 92
ZF-LRAT                           D----LLEVPRTLFTHFGIYLGDNKVAHLMPDILPVLTSNKSHLQNVVTN 91
HRev107-Mouse                     D----LIEIFRPMYRHWAIYVGDGYVIHLAPPSEVAGAGAAS-------- 49
HREV107-RAT                       D----LIEIFRPMYSHWAIYVGDGYVIHLAPPSEIPGAGAAS-------- 47
HRev107-3                         D----LIEIFRPFYRHWAIYVGDGYVVHLAPPSEVAGAGAAS-------- 49
TIG3                              D----LIEIFRLGYEHWALYIGDGYVIHLAPPSEYPGAGSSS-------- 49
Echovirus23                       K----LAYLDRGFYKHYGIIVG-GYVYQLDSDDIFKTA------------ 86
HumanParechovirus1                K----LAYLDRGFYKHYGIIVG-DHVYQLDSDDIFKTA------------ 78
HumanParechovirus2                K----LAYLDRGFYKHYGIVVG-DDVYQLDSDDIFKTA------------ 77
Avian-encephalomyelitis-virus     D----IVSCSGEKAKHFGVYVG-DGVVHVDPEGNATNWFMKR-------- 76
EGL26                             DEVFCEVNVSGVKFYHSGIYAGDGMCYHFVCDAQESESFADALAVFSG-- 198
Aichivirus                        DDRVYIVRAQRPTYVHWAIRKVAPDGSAKQISLSRSGIQALV-------- 48

Human-LRAT                        KRLILGVIVKVASIRVDTVEDFAYGANILVNHLDESLQKKALLNEEVARR 144
Bovine-LRAT                       KRLILGVIGRVASIRVDTVEDFAYGAEILVNHLDRSLKKKALLNEEVAQR 144
Mouse-LRAT                        KRLLLGVICKVASIRVDTVEDFAYGADILVNHLDGTLKKKSLLNEEVARR 144
Rat-LRAT                          KRLLPGVICKVASIRVDTVEDFAYGADILVNHLDETLKKKSLLNEEVARR 144
XL-LRAT                           KRLIMGVLAKIASIRVDSVQDFAYGGNILVNHMDKSFKTKPLTNEEVARR 142
ZF-LRAT                           KRLLLGVLYKYASVRVDTVEVFAYGSNILLNTMDTTLRKQPLAAEEVARR 141
HRev107-Mouse                     ---IMSALTDKAIVKKELLCHVAGKDKYQVNNKHDEEYT-PLPLSKIIQR 95
HREV107-RAT                       ---IMSALTDKAIVKKELLRDVAGKDKYQVNNKHDKEYT-PLPLNKIIQR 93
HRev107-3                         ---VMSALTDKAIVKKELLYDVAGSDKYQVNNKHDDKYS-PLPCSKIIQR 95
TIG3                              ---VFSVLSNSAEVKRGRLEDVVGGCCYRVNNSLDHEYQ-PRPVEVIISS 95
Echovirus23                       ------LTGKARFTKTRLTPDWIVEEECELDYFRVKYLESSVNSEHIFS- 129
HumanParechovirus1                ------LTGKAKFTKTKLTSDWVIEEECELDYFRIKYLESAVDSEHIFS- 121
HumanParechovirus2                ------LTGKAKFTKTRLTPDWVVEEECELDYFRIKYLESSVNSEHIFS- 120
Avian-encephalomyelitis-virus     ---------KATVKKSKNLDKWCFALSPRIDRTLICETANLMVGREVEYD 117
EGL26                             -----ASAHVVYDTWFEFVYALVEVSDVPPKIFRASHPLICRSGEQVVKY 243
Aichivirus                        -----ALEPPEGEPYLEILPSHWTLAELQLGNKWEYS------------- 93

Human-LRAT                        AEKLLG-FTPYSLLWNNCEHFVTYCRYGTPISPQSDKFCETVKIIIRDQR 193
Bovine-LRAT                       AEKLLG-ITPYSLLWNNCEHFVTYCRYGTPISPQADKFCENVKIIIRDQR 193
Mouse-LRAT                        AEQQLG-LTPYSLLWNNCEHFVTYCRYGSRISPQAEKFYDTVKIIIRDQR 193
Rat-LRAT                          AEQQLG-LTPYSLLWNNCEHFVTYCRYGSPISPQAEKFHETVKILIRDQR 193
XL-LRAT                           AEKLVG-STPY-LLWNNCEHFVTYCRYGMPVSFQTEKFCETVKKIIRDRR 190
ZF-LRAT                           AEKLVG-HFTYSLMWNNCEHFVTYCRYGTAVSLQTDQFCESLKSIIRDQR 190
HRev107-Mouse                     AERLVGQEVLYRLTSENCEHFVNELRYGVPRSDQ----------VRDAV 134
HREV107-RAT                       AEELVGQEVLYRLTSENCEHFVNELRYGVPRSDQ----------VRDTV 132
HRev107-3                         AEELVGQEVLYKLTSENCEHFVNELRYGVARSDQ----------VRDVI 134
TIG3                              AKEMVGQKMKYSIVSRNCEHFVAQLRYGKSRCKQ----------VEKAK 134
Echovirus23                       ------------VDSNCETIAKDIFGTHTLSQH------------QAI 153
HumanParechovirus1                ------------VDKNCETIAKDIFGTHTLSQH------------QAI 145
HumanParechovirus2                ------------VDNNCETIAKDIFGSHSLSQH------------QQI 144
Avian-encephalomyelitis-virus     ------------IFVKNCETYARGIASGDYGTKEGEK--------WKTLL 147
EGL26                             AEHLQRELENYDIRRCNCQHFSSECSTGVPFSYD----------MTSNF 282
Aichivirus                        A-------T------NNCTHFVSSI-TGESLPN----------------T  99

Human-LRAT                        SVLASAVLGLASIVCTGLVSYTTLPAIFIPFFLWMAG- 230
Bovine-LRAT                       SVLASAVLGLASIFCLGLTSYTTLPAIFIPFLLWMAG- 230
Mouse-LRAT                        SSLASAVLGLASIVYTGLASYMTLPAICIPFCLWMMSG 231
Rat-LRAT                          SCLASAVLGLVSIIYTGLASYMTLPAVCIPFCLWMMSG 231
XL-LRAT                           SALLSAAIGMASVLCMGFGLCTILPSFFITFTLWMAS- 227
ZF-LRAT                           SILLTTVIGNLSMFFVGIAPSTALPTFIIPFILWMAG- 227
HRev107-Mouse                     KAVGIAGVGLAALGLVGVMLSRNKKQKQ---------- 162
HREV107-RAT                       KVATVTGVGLAALGLIGVMLSRNKKQKQ---------- 160
HRev107-3                         IAASVAGMGLAAMSLIGVMFSRNKRQKQ---------- 162
TIG3                              VEVGVA-TALGILVVAGCSFAIRRYQKKATA------- 164
Echovirus23                       GLVGAILLTAGLMSTIKTPVNATTIKEFFNHAIDGDEQ 191
HumanParechovirus1                GLVGTILLTAGLMSTIKTPVNAVTIKEFFNHAIDGDEQ 183
HumanParechovirus2                GLIGTILLTAGLMSTIKTPVNPTTIKEFFNHAIEGDEQ 182
Avian-encephalomyelitis-virus     SAVGVAAMTTTMMAMRHELLDTSLTKLPQKVGEVT--- 182
EGL26                             KYLACTVLKPTSTVVNAMTRPNRDRSSFASSSTSS--- 317
Aichivirus                        GFSLALGIGALTAIAASAAVAVKALPGIRRQGLLTLSA 137
```

[a] Multiple sequence alignment of the LRAT family was performed by using CLUSTAL W 1.82 (http://www.ebi.ac.uk/clustalw/). Fully conserved His, Tyr, and Cys are in red. Accession numbers are as follows: human LRAT (GP:AF 071510), bovine LRAT (GP:AF 275344), mouse LRAT (GP:AF 255061), rat LRAT (GP:AF 255060), mouse Hrev107 (AAH24581), rat Hrev107 (X76453), human Hrev107-3 (P53816), tazarotene-induced gene protein (TIG3) (AF060228), echovirus23, human parechovirus1 (L02971), human parechovirus2 (AJ005695), avian-encephalomyelitis-virus (AJ225173), EGL26 (NP493652), and Aichivirus (AB010145).

These residues would be expected to appear among the conserved residues in the extended LRAT family (Scheme 3). The first residue in question is C161, which is fully conserved in the extended LRAT family, and is also found in a strongly conserved context (NCEH) (Scheme 3) (*9*, *13*). Substitution mutations at C161 are catalytically inert (*9*, *16*), and C161 is alkylated by the specific LRAT affinity labeling agent BRCA. That C161 is the residue responsible for the

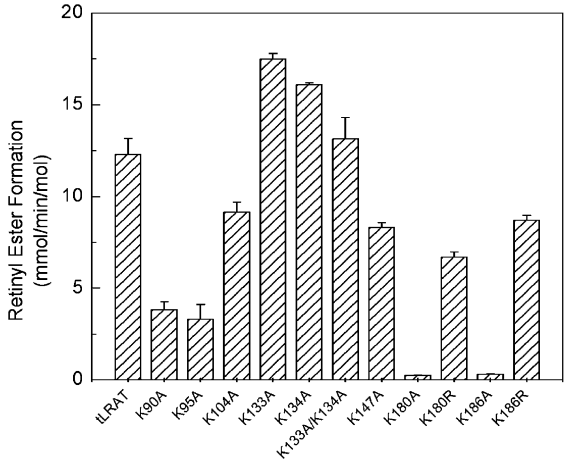

FIGURE 4: Retinyl ester formation by tLRAT and K → A/R mutants. Experimental details are described in the Methods section. For the activity assay of tLRAT and the mutants, the reaction mixture includes 100 mM Tris-HCl buffer, 1 mM EDTA, 1 mM DTT, 5 μM tLRAT or mutant, and 240 μM DPPC/BSA (0.6%). The reaction was initiated by adding all-*trans*-retinol (0.2 μM), incubated at room temperature for 10 min. All experiments were done in triplicate, and the errors are shown as error bars in the figure.

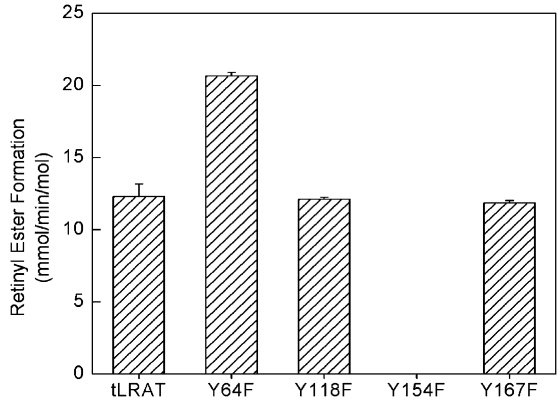

FIGURE 5: Retinyl ester formation by tLRAT and Y → F mutants. The experimental details are described in the Methods section. For the activity assay of tLRAT and the mutants, the reaction mixture includes 100 mM Tris-HCl buffer, 1 mM EDTA, 1 mM DTT, 5 μM tLRAT or mutant, and 240 μM DPPC/BSA (0.6%). The reaction was initiated by adding all-*trans*-retinol (0.2 μM), incubated at room temperature for 10 min. All experiments were done in triplicate, and the errors are shown as error bars in the figure.

pK_a appearing in the pH vs rate profile is reasonable, given a value of 8.22. However, it is well-known that active site pK_a values for amino acid residues may deviate markedly from values obtained from model studies, and consequently additional experimental evidence is useful here (*22*, *23*). With chemically reactive amino acids, such as Cys, it is possible to chemically titrate them as a function of pH (*22*, *23*). Under ideal circumstances, the midpoint of the curve subsequently obtained should correlate with the pK_a value obtained

Scheme 4: LRAT Mechanism Showing the Involvement of H60, Y154, and C161

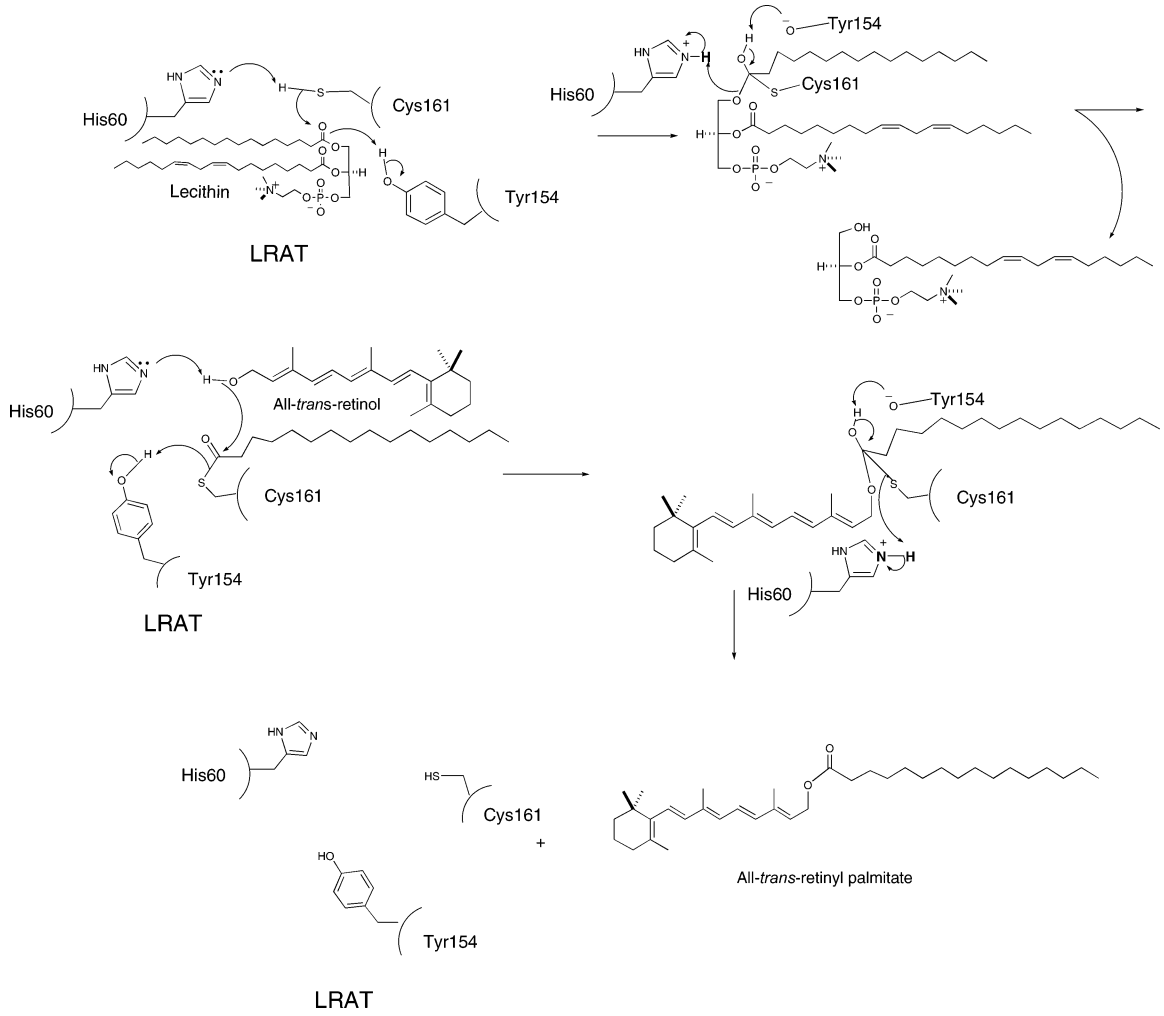

independently from the pH vs rate profile (*22*, *23*). BRCA is used for this purpose in the studies described here. It is already known that BRCA uniquely alkylates C161 of tLRAT and irreversibly inactivates the enzyme as a consequence of this (*9*). The extent of tLRAT alkylation by BRCA can be quantitatively measured using a conjugated avidin derivative to detect the biotin moiety. Titration with BRCA reveals a pK_a for C161 to be quite similar to the ascending pK_a in the pH vs rate profile (*16*). An exact match of pK_a values would not be expected given the different chemical reactions being compared in the enzymatic processing and in the titration reaction. These data leave little doubt that C161 is involved in a rate-limiting step in the reactions catalyzed by LRAT.

The situation with the descending pK_a in the profile of 9.95 is somewhat more complex. First, this is a very high pK value. However, it is known that the optimal pH for LRAT is also high (approximately 8.5) (*16*). Essentially two amino acids, Lys and Tyr, come to mind as candidates. Lysine could be easily ruled out as a candidate because none of the weakly conserved Lys residues proved to be essential for tLRAT function. Tyrosine proved to be more interesting because of the seven residues in LRAT, only Y154 proved to be essential for catalysis. Interestingly, Y154 is the most conserved of all of the Tyr residues, appearing in all of the close LRAT homologues (Scheme 3) (*9*). Y154 appears in all of the LRAT isoforms, in the four tumor suppressor proteins (HRev107-mouse, HRev107-rat, HRev107-3, TIG3), and in EGL26, a protein that mediates morphogenesis in *C. elegans* (*12*). It does not appear in the homologous putative viral proteases, suggesting a possible divergence of mechanism in this group (Scheme 3) (*24*). This group does absolutely conserve C161 and H60 (*9*). In the LRAT subgroup possessing an Y154 homologue, this amino acid is likely to be acting as an acid. This is consistent with Y154 being responsible for the descending limb of the pH vs rate profile, as suggested here. In the case of LRAT, a likely mechanistic scenario incorporating C161, H60, and Y154 is shown in Scheme 4.

In summary, the experiments reported here show that C161 is the residue responsible for the pK_a = 8.22 observed in the pH vs rate profile for LRAT. It is likely that Y154 is responsible for the higher pK_a observed here. Therefore, an important subgroup of the LRAT family of enzymes possesses three essential residues, H60, Y154, and C161, and however these proteins are folded, these three residues must be part of the active site. Further studies will be required to reveal the chemical mechanisms of action of this novel family of enzymes.

REFERENCES

1. MacDonald, P. N., and Ong, D. E. (1988) Evidence for a lecithin-retinol acyltransferase activity in the rat small intestine, *J. Biol. Chem. 263*, 12478−12482.
2. Barry, R. J., Cañada, F. J., and Rando, R. R. (1989) Solubilization and partial purification of retinyl ester synthetase and retinoid isomerase from bovine ocular pigment epithelium, *J. Biol. Chem. 264*, 9231−9238.
3. Saari, J. C., and Bredberg, D. L. (1989) Lecithin:retinol acyltransferase in retinal pigment epithelial microsomes, *J. Biol. Chem. 264*, 8636−8640.
4. Rando, R. R. (2001) The biochemistry of the visual cycle, *Chem. Rev. 101*, 1881−1896.
5. Gollapalli, D. R., and Rando, R. R. (2003) All-trans-retinyl esters are the substrates for isomerization in the vertebrate visual cycle, *Biochemistry 42*, 5809−5818.
6. Moiseyev, G., Crouch, R. K., Goletz, P., Oatis, J., Redmond, T. M., and Ma, J.-X. (2003) Retinyl esters are the substrate for isomerohydrolase, *Biochemistry 42*, 2229−2238.
7. Batten, M. L., Imanishi, Y., Maeda, T., Tu, D., Moise, A. R., Bronson, D., Possin, D., Van Gelder, R. N., Baehr, W., and Palczewski, K. (2004) Lecithin-retinol acyltransferase is essential for accumulation of all-trans-retinyl esters in the eye and in the liver, *J. Biol. Chem. 279*, 10422−10432.
8. Zolfaghari, R., and Ross, A. C. (2000) Lecithin:retinol acyltransferase from mouse and rat liver. CDNA cloning and liver-specific regulation by dietary vitamin a and retinoic acid, *J. Lipid Res. 41*, 2024−2034.
9. Jahng, W. J., Xue, L., and Rando, R. R. (2003) Lecithin retinol acyltransferase is a founder member of a novel family of enzymes, *Biochemistry 42*, 12805−12812.
10. Sers, C., Emmenegger, U., Husmann, K., Bucher, K., Andres, A. C., and Schafer, R. (1997) Growth-inhibitory activity and down-regulation of the class II tumor-suppressor gene H-rev107 in tumor cell lines and experimental tumors, *J. Cell Biol. 136*, 935−944.
11. Hajnal, A., Klemenz, R., and Schafer, R. (1994) Subtraction cloning of H-rev107, a gene specifically expressed in H-ras resistant fibroblasts, *Oncogene 9*, 479−490.
12. Hanna-Rose, W., and Han, M. (2002) The *Caenorhabditis elegans* EGL-26 protein mediates vulval cell morphogenesis, *Dev. Biol. 241*, 247−258.
13. Hughes, P. J., and Stanway, G. (2000) The 2A proteins of three diverse picornaviruses are related to each other and to the H-rev107 family of proteins involved in the control of cell proliferation, *J. Gen. Virol. 81*, 201−207.
14. Shi, Y.-Q., Hubacek, I., and Rando, R. R. (1993) Kinetic mechanism of lecithin retinol acyl transferase, *Biochemistry 9*, 1257−1263.
15. Furuyoshi, S., Shi, Y.-Q., and Rando, R. R. (1993) Acyl group transfer from the sn-1 position of phospholipids in the biosynthesis of n-dodecyl palmitate, *Biochemistry 32*, 5425−5430.
16. Mondal, M. S., Ruiz, A., Bok, D., and Rando, R. R. (2000) Lecithin retinol acyltransferase contains cysteine residues essential for catalysis, *Biochemistry 39*, 5215−5220.
17. Storer, A. C., and Menard, R. (1994) Catalytic mechanism in papain family of cysteine peptidases, *Methods Enzymol. 244*, 486−500.
18. Bok, D., Ruiz, A., Yaron, O., Jahng, W. J., Ray, A., Xue, L., and Rando, R. R. (2003) Purification and characterization of a transmembrane domain-deleted form of lecithin retinol acyltransferase, *Biochemistry 42*, 6090−6098.
19. Nesnas, N., Rando, R. R., and Nakanishi, K. (2002)Synthesis of biotinylated retinoids for cross-linking and isolation of retinol binding proteins, *Tetrahedron 58*, 6577−6584.
20. Ruiz, A., Winston, A., Lim, Y.-H., Gilbert, B. A., Rando, R. R., and Bok, D. (1999) Molecular and biochemical characterization of lecithin retinol acyltransferase, *J. Biol. Chem. 274*, 3834−3841.
21. Jahng, W. J., David, C., Nesnas, N., Nakanishi, K., and Rando, R. R. (2003) A cleavable affinity biotinylating agent reveals a retinoid binding role for RPE65, *Biochemistry 42*, 6159−6168.
22. Mellor, G. W., Patel, M., Thomas, E. W., and Brocklehurst, K. (1993) Clarification of the pH-dependent kinetic behaviour of papain by using reactivity probes and analysis of alkylation and catalysed acylation reactions in terms of multihydronic state models: implications for electrostatics calculations and interpretation of the consequences of site-specific mutations such as Asp-158-Asn and Asp-158-Glu, *Biochem. J. 294*, 201−210.
23. Knowles, J. R. (1976) The intrinsic pK_a-values of functional groups in enzymes: improper deductions from the pH-dependence of steady-state parameters, *CRC Crit. Rev. Biochem. 4*, 165−173.
24. Anantharaman, V., and Aravind, L. (2003) New connections in the prokaryotic toxin-antitoxin network: relationship with the eukaryotic nonsense-mediated RNA decay system, *Genome Biol. 4*, R11−R11.12.

BI049556F